GEOPHYSICAL RESEARCH LETTERS, VOL. 34, L09101, doi:10.1029/2006GL028829, 2007

Absorption of MARSIS radar signals: Solar energetic particles and the daytime ionosphere

Jared R. Espley,[1] William M. Farrell,[1] David A. Brain,[2] David D. Morgan,[3] Bruce Cantor,[4] Jeffrey J. Plaut,[5] Mario H. Acuña,[1] and Giovanni Picardi[6]

Received 20 November 2006; revised 1 March 2007; accepted 29 March 2007; published 2 May 2007.

[1] We present observations from the subsurface sounding mode of the MARSIS instrument onboard Mars Express that imply radar wave absorption because of increased amounts of ionization in the upper Martian atmosphere during the fall of 2005. On at least two occasions these radar disruptions lasted for several days and we find that these periods are correlated with periods when other instruments indicate elevated levels of solar energetic particles. Another disruption lasted for over a month and we find that it was likely caused by a combination of solar activity and observing through the daytime ionosphere. There is no evidence in the present results for the constant ionospheric layer predicted to be created by the normal infall of cosmic dust, although the effects of enhanced infall during meteor showers remains uncertain. The effects of dust activity also remain uncertain but will be tested during the 2007 dust season. **Citation:** Espley, J. R., W. M. Farrell, D. A. Brain, D. D. Morgan, B. Cantor, J. J. Plaut, M. H. Acuña, and G. Picardi (2007), Absorption of MARSIS radar signals: Solar energetic particles and the daytime ionosphere, *Geophys. Res. Lett.*, *34*, L09101, doi:10.1029/2006GL028829.

1. Introduction

[2] The Martian ionosphere has been the subject of many studies over the years (see *Withers and Mendillo* [2005] and *Mendillo et al.* [2003, Table 1] for a recent set of references), but many important questions remain about its nature. The Mars Advanced Radar for Subsurface and Ionospheric Sounding (MARSIS) experiment onboard Mars Express (MEX) [*Picardi et al.*, 2005; *Gurnett et al.*, 2005] was designed, in part, to provide unprecedented radio wavelength investigations of the ionosphere. In this work, we examine MARSIS measurements to investigate the causes of the radar signal "blackout" periods when ground reflections from the subsurface sounding mode disappeared in the second half of 2005. We investigate possible causes such as variable ionization layers created by cometary-derived meteoric material, planetary dust storm activity, crustal magnetic fields, diurnal cycles of ionization, and solar activity. We find that the shorter blackout periods are well correlated with solar activity and that the longest period of blackouts was likely associated with the diurnal cycle of ionization.

2. Data

[3] The MARSIS instrument consists of a 40 m antenna transmitter/receiver system. After some initial concerns regarding antenna deployment, the 40 m tip-to-tip system was successfully unfurled in mid-June 2005. MARSIS has two very different modes, both of which operate near periapsis [*Safaeilini et al.*, 2003]. These modes are so very different that the instrument can really be considered two separate sounder systems. To probe the ionosphere via active ionospheric sounding (AIS mode), MARSIS transmits a continuous wave pulse of $\sim$91 μsec duration in 160 frequency steps between 100 kHz and 5.6 MHz. The second MARSIS mode is specifically for sounding the subsurface (SS mode), with the MARSIS transmitter emitting a broad 1 MHz bandwidth chirp pulse tunable to 4 distinct bands: 1.3–2.3 MHz, 2.5–3.5 MHz, 3.5–4.5 MHz, and 4.5–5.5 MHz.

[4] The SS mode is very sensitive to the timing of the ground detection. Due to the desire to probe the subsurface with $<$1 μsec temporal resolution, the onboard SS system does not return a large volume of data following a transmission, but instead predicts the time of the ground return pulse and returns data in a relatively narrow $\sim$180 μsec temporal window centered about the predicted pulse return. This data selection process guarantees that high-resolution subsurface reflections detected in time periods immediately following the ground pulse are captured. In contrast, the receiver in AIS mode transmits and then listens to all return signals in a longer but less resolved $\sim$7 msec temporal window. The resolution of the AIS mode product is $\sim$91 μsec, whereas the resolution of the SS mode is $\sim$0.35 μsec (or a factor of 300 different). Thus, SS mode returns a smaller temporal window, but this window is centered specifically on the ground return pulse. Any modifications in the ground return pulse should be noticeable in the finer resolved, ground pulse-centered SS data format.

[5] MARSIS data are typically displayed as echograms showing power received as a function of delay time (equivalent to distance beneath the satellite, shown on the ordinate) and time (equivalent to distance along the ground track, shown on the abscissa). Figure 1a shows a typical SS return from orbit 1874 (1 Jul 2005). The return from the surface is clearly seen along with hints of subsurface features. Additionally, the abrupt change in surface eleva-

[1]NASA Goddard Space Flight Center, Greenbelt, Maryland, USA.
[2]Space Sciences Laboratory, University of California, Berkeley, California, USA.
[3]Department of Physics and Astronomy, University of Iowa, Iowa City, Iowa, USA.
[4]Malin Space Science Systems, San Diego, California, USA.
[5]Jet Propulsion Laboratory, California Institute of Technology, Pasadena, California, USA.
[6]Infocom Department, La Sapienza University of Rome, Rome, Italy.

0094-8276/07/2006GL028829$05.00

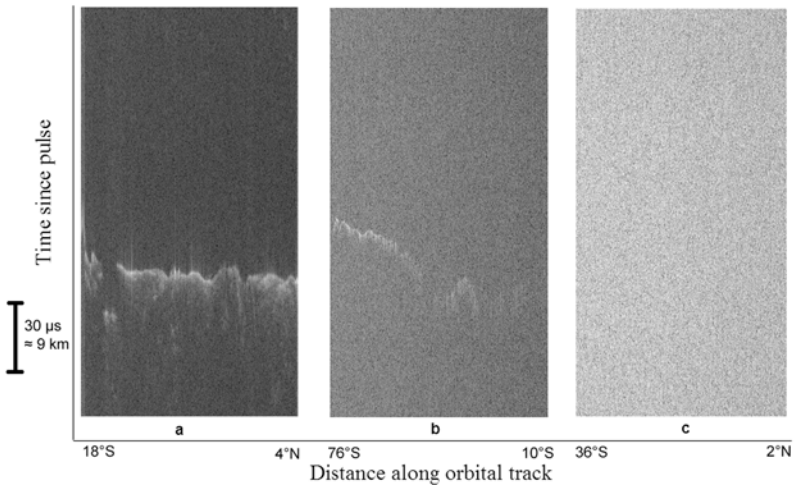

Figure 1. MARSIS subsurface sounder radar returns from three different orbits displayed as delay vs. time echograms with the grey scale representing the received radar intensity. (a) A typical return. (b) A marginal return. (c) A poor return.

tion at Valles Marineris is seen near the beginning of the return. Figure 1b shows a similar return from orbit 2211 (3 Oct 2005) but in this case the surface return is barely discernible and there are no details present. Figure 1c shows an example of what we are terming a ''blackout''; the SS return from orbit 1986 (1 Aug 2005) shows no evidence for any ground return. The grey scale is normalized to the maximum intensity of each individual echogram but represents a maximum difference of approximately 60 dB.

[6] Figure 2 shows a variety of time series datasets that encompass the times when these disruptions occurred. Figure 2a shows a qualitative evaluation of a series of data similar to Figure 1. Orbits showing data similar to Figure 1a (a good ground return and possibly some other details

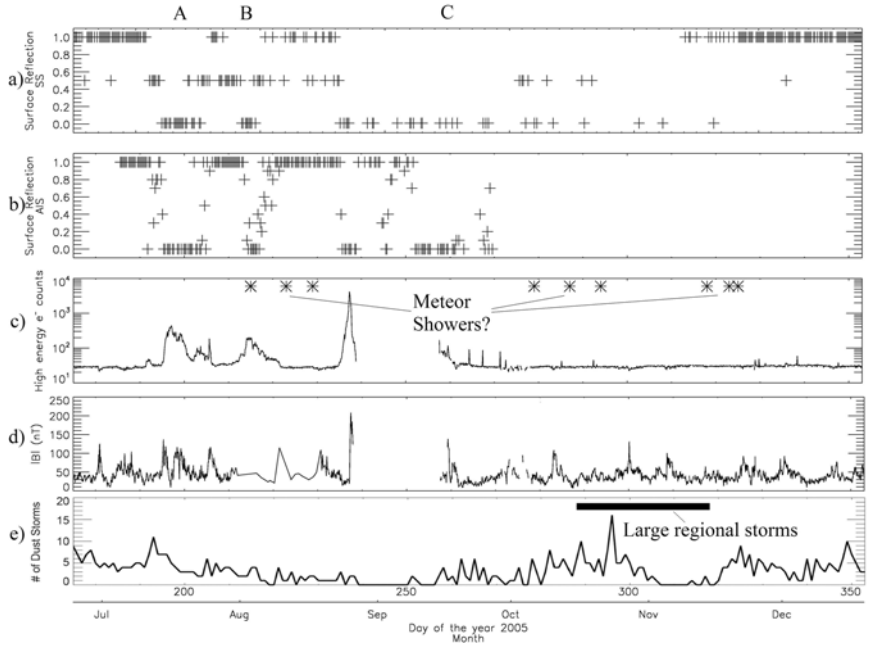

Figure 2. Time series data from the period of radar disruption. (a) A qualitative assessment of whether the Subsurface Sounder showed a clear ground signal (1 for very clear, 0.5 for faint or strongly distorted, and 0 for a complete ''blackout'' like Figure 1c). (b) A similar dataset from the Active Ionospheric Sounder experiment [from *Morgan et al.*, 2006]. (c) The total countrate in the 10–21 keV energy channels from the MGS Electron Reflectometer. These electrons mainly represent high energy (>20 MeV) particles. The asterisks show when Mars crossed the path of a comet. (d) The average subsolar magnetic field magnitude as measured by the MGS magnetometer. (e) The total number of dust storms observed in MOC images from across the planet. The black bar represents a period when several large regional dust storms developed.

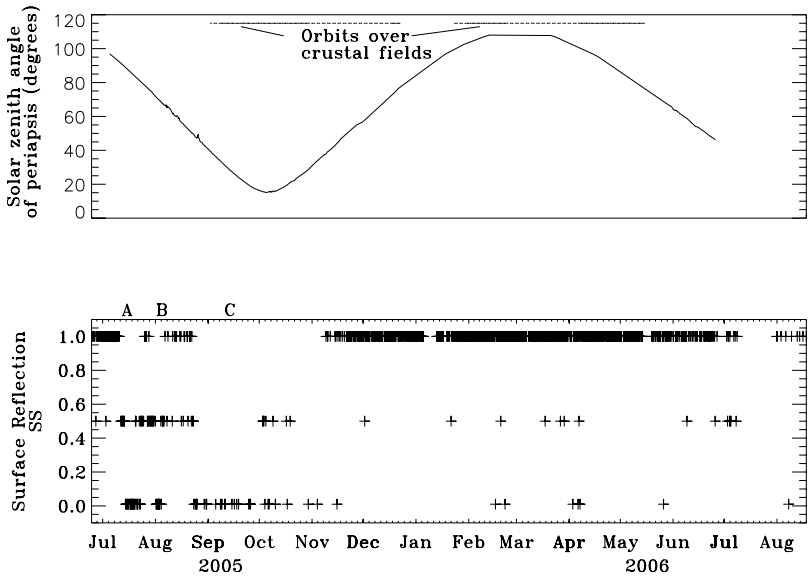

Figure 3. Time series comparing the MARSIS blackouts with the MEX periapses. (top) The solar zenith angles of the periapses. The dots at the top show when a periapsis occurred over the region of most prominent crustal magnetic fields. (bottom) The subsurface data quality index like in Figure 2a (although for a longer time period so a comparison with Figure 3, top, can be easily made).

discernible) are rated as 1, orbits like Figure 1b (a weak ground return and no discernible details) are rated as 0.5, and orbits like Figure 1c (no discernible ground return) are rated as 0. Figure 2b shows a similar "data quality" index for the AIS measurements from *Morgan et al.* [2006]. They also rated their ionograms as 1 for having a visible surface and 0 for not having a visible surface and then averaged over ten orbits sampled around 850 km to get values between 0 and 1.

[7] The next few panels show data for comparison from Mars Global Surveyor (MGS) for the same time period. Figure 2c shows the count rate averaged over two hours in the three highest energy channels of the Electron Reflectometer [*Mitchell et al.*, 2001] experiment onboard MGS. These bins nominally only record electrons with energy between 10 and 21 keV, but since such particles are typically rare it is expected that the signal in this channel is usually dominated by high energy particles (10's of MeV) that penetrate the instrument casing and strike the detector. Thus these energy bins give an estimate of the background high energy particle flux at Mars [*Brain*, 2007]. Also shown as asterisks are the times that Mars crossed the orbital path of comets and hence could in principle encounter the dust stream laid down by these comets (see the discussion below). Figure 2d uses MGS magnetometer (MAG) [*Acuña et al.*, 2001] data to show the average subsolar magnetic field magnitude [*Crider et al.*, 2003; *Brain et al.*, 2005] at Mars for the time period of interest. Large increases in $|B|$ are usually associated with enhanced solar wind activity at Mars [*Crider et al.*, 2005]. Similar data for the entire period that MGS has been in its mapping orbit (1999–present) are publicly available at the time of writing at http://sprg.ssl.berkeley.edu/~brain/rsrch/subsolfield.html. The data gap shown in Figures 2c and 2d for late Aug. and early Sep. was caused when MGS went into safe mode; this was presumably caused by the solar energetic particles recorded at the beginning of this interval (see discussion below). The bottom panel (Figure 2e) shows the total number of dust storms observed daily (in Mars Orbital Camera (MOC) global images, taken at a resolution of 7.5 km/pixel [*Cantor et al.*, 2002]) across all of Mars as a function of day of the year. The dark bar at the top extending from day 288–318 is the duration of a large regional dust event and the dust cloud it generated.

[8] In order to investigate the effects of the orbital evolution of MEX on the blackouts, Figure 3 shows results relating to the geographic locations and the relative local time of day for the periapses. The top panel shows a time series of the solar zenith angles (SZAs) of the periapses. Dots near the top of the panel indicate orbits when the periapsis was within the region of the largest crustal magnetic fields (latitudes 10 to 80°S and longitudes 140 to 220°E [*Connerney et al.*, 2001]). Note that although the periapsis latitude varies smoothly with time the periapsis longitude changes drastically from orbit to orbit and hence periapses near the crustal fields are intermingled with periapses away from the crustal fields for long stretches of time. The bottom panel is similar to Figure 2a except that it shows a longer time period of the data quality index of the MARSIS SS echograms. This allows comparisons to be made with a complete cycle of orbital evolution but the temporal scale is more compressed than in Figure 2.

3. Discussion

[9] What caused the variation in ground returns as shown in Figure 1? In order to answer this, we note first that at least two types of disruptions appear to be present. The first are disruptions that last several days; Figure 2a shows one period (which we call event "A") of complete disruptions (both MARSIS datasets go to zero) that starts on 14 July and lasts for about 9 days (until approximately Jul 23).

A similar event (event "B") begins on 1 August and lasts until about 4 August. Another, longer event (event "C") starts around Aug. 23 and appears to end in early November. Unfortunately, due to spacecraft operation constraints (other instruments were using much of the power and data download bandwidth available), we have only very limited data in October (see Figure 2a) but the anomalously long duration of event C appears clearly in the dataset. We consider here several explanations for these events but in all cases we start with the assumption that some mechanism has increased the ionization at altitudes lower than the observation and thereby disrupted the ground return of the MARSIS signal.

3.1. Meteoric Effects

[10] *Pesnell and Grebowsky* [2000] and *Molina-Cuberos et al.* [2003] suggested that, due to meteoric infall and subsequent photoionization, an ionospheric layer of magnesium and iron ions should form around 80 km in the Martian ionosphere. This material was assumed to originate from the steady state infall from micrometeoroids that are common throughout the solar system (the unfortunately named "sporadic" component). *Witasse et al.* [2001] followed up on this work to show that such a layer would cause attenuations as large as 360 dB at 1.8 MHz and 50 dB at 5 MHz. Thus they predicted that MARSIS, which operates in these frequency ranges, would experience significant attenuation. The results shown here and in other work [e.g., *Picardi et al.*, 2005] demonstrate that this attenuation is not present.

[11] *Pesnell and Grebowsky* [2000] did note that the effects from passing through the dust stream left by a recent passage of a short period comet should cause a factor of 2–3 increase in the observed densities but did not consider such short term effects further in their model. A recent model by *McNeil et al.* [2001] shows that for the terrestrial ionosphere an order of magnitude increase in metallic ion density can be expected for an ordinary meteor shower, and, for a strong meteor storm, the densities of normal ionospheric ions can be temporarily overshadowed by metallic ions. Thus, it is possible that events such as large meteor showers and storms, which represent periods of highly elevated rates of meteoric infall, may produce significant and time variable layers in the Martian ionosphere [cf. *Patzold et al.*, 2005]. Therefore, we looked for all known Mars-crossing comets to see if there was a correlation with the MARSIS blackouts. *Treimann and Treimann* [2000] identify 29 Jupiter Family Comets (JFCs) in their Table 1 and add 171P/Spahr in the text. *Selsis et al.* [2004] adds two more JFCs to bring the known total to 32. Additionally, there are 3 Mars-crossing Halley type comets [*Treimann and Treimann*, 2000]. Using the JPL Small-Body Database Browser at http://ssd.jpl.nasa.gov/sbdb.cgi, we found that of these 35, only 9 had tracks that passed within 0.1 AU of Mars (a necessary but not sufficient criterion for meteor showers [*Christou*, 2005]) during the period from July to November of 2005. Figure 2 shows that while several cometary track encounters occur during blackout events, none of these correspond exactly with the onset of the blackout events. Hence, while any of the comets mentioned could conceivably cause meteor showers at Mars and could thus affect MARSIS via increased atmospheric ionization, we find no obvious connection between cometary material and the 2005 MARSIS blackouts. However, in future work we hope to use detailed models [e.g., *Vaubaillon et al.*, 2005] to make more precise predictions of when Martian meteor showers might occur and to make observations of any ionospheric effects during these time periods.

3.2. Dust Activity

[12] Turning to other mechanisms, it is plausible that dust activity could alter the ionosphere [*Bougher et al.*, 2004; *Wang and Nielsen*, 2003] to change its absorption and reflection characteristics. Terrestrial polar mesosphere summer echoes of various radar investigations have been attributed to charged aerosols present in the Earth's polar mesosphere [*Cho and Rottger*, 1997]. The time period under consideration is at a planetocentric solar longitude L_s = 250–300, which is during the main Mars dust season (although slightly past the peak [cf. *Liu et al.*, 2003, Figure 10]). However, comparing Figures 2a and 2e, we find that the number of dust storms in MOC images does not correlate particularly well with the MARSIS blackouts. There is a correlation between the onset of event A with an increase in the number of dust storms but this increase does not appear to be statistically significant. No dust activity is associated with event B. The series of large regional storms starting in late Oct. (indicated by the black bar in Figure 2e) does occur near the end of the event C, possibly prolonging the blackout period although dust activity is clearly not the original and primary cause for the blackouts. Hence, any correlation between the blackouts and dust events is inconclusive, at best. Fortunately, the seasonal dust activity will peak again in early 2007, so we anticipate being able to test possible dust effects on MARSIS results at that time.

3.3. SEP Effects

[13] However, Figure 2 does show that events A, B, and C all start at nearly the exact same time as there are sharp increases in the solar activity as recorded by the MAG/ER experiment on MGS (Figures 2c and 2d). *Morgan et al.* [2006] first noted this correlation in their study using the MARSIS AIS dataset, and they attributed the blackouts to absorption of the radar waves by layers of increased ionization created by solar energetic particles (SEPs). The results presented here reinforce this idea although the length of the blackouts is significantly longer than other previously observed ionization events associated with solar activity. For example, radio science results from both MGS and MEX [*Mendillo et al.*, 2006; *Patzold et al.*, 2005] find sudden ionospheric disturbances and low altitude ionospheric layers that have timescales of hours or at most a day. Likewise, *Crider et al.* [2005] and *Espley et al.* [2005] found the huge coronal mass ejections of October–November 2003 had effects on the Martian upper atmosphere that lasted on the timescale of a few days. Nonetheless, solar energetic particle effects on the terrestrial ionosphere have been seen to last as long as 20 days [see *Patterson et al.*, 2001, Figure 3] although effects of a few days are more typical. Thus, given the good correlation with MGS solar activity proxy data, we agree with *Morgan et al.* [2006] in considering solar activity to be the primary cause of the blackouts that lasted for days (i.e. events A, B, and the first few days of event C).

3.4. Anomalous Duration of Event C: The Diurnal Effect

[14] However, we are still left to try to explain the longest event (event C) which, by the SS results shown here, lasted for two months or more. Looking at Figure 3 (top), it is clear that crustal magnetic fields did not, in general, significantly affect MARSIS's ability to see the ground since there are intervals in which the blackouts occur over the crustal fields and intervals in which the blackouts occurred nowhere near the crustal fields. Conversely, it would appear that the diurnal cycle does affect the MARSIS results as we can see that for most of event C that the observations were taken when periapses were in the daytime and were far from either dusk or dawn. In other words, the SS mode appears to blackout when MARSIS is transmitting through the dense portion of the dayside ionosphere. While some ground return signal attenuation was expected, a complete blackout was not anticipated [*Safaeilini et al.*, 2003]. The peak plasma frequency on the dayside is ~4 MHz [*Gurnett et al.*, 2005] and 5 MHz signals would be expected to return from ground reflection, albeit distorted. The blackout period later in event C could result from either complete attenuation of the signal or possibly the inability of MARSIS' SS mode to autonomously lock onto a ground pulse (due to an extended group delay or smearing of the pulse). Thus, the prolonged duration of event C is a result of the combination of an SEP-triggered event that preceded a long-term diurnal related attenuation period. The fact that a similar blackout did not occur in July 2006 (when the periapses returned to similar SZAs) indicates that the diurnal effect alone may not be sufficient to completely disrupt the radar returns. The role of the regional dust storm also occurring during the period of event C is ambiguous, but will be tested during the major storm season in 2007.

4. Conclusions and Future Work

[15] In summary, we find that solar energetic particles and the daily ionization cycle create time variable layers in the Martian ionosphere that scatter or absorb high frequency radar signals such as MARSIS. Additionally, we find no evidence for a constant ionospheric meteoric layer although we hope to further investigate other physical mechanisms for ionospheric variation including meteor shower impacts and dust activity.

[16] **Acknowledgments.** J. Espley was supported as a NASA postdoctoral fellow at Goddard Space Flight Center. Members of the MEX and MGS science and engineering teams worked hard to produce the data used in this work; their efforts are greatly appreciated. Useful information about the orbits of near Mars comets was found at http://ssd.jpl.nasa.gov/sbdb.cgi including the Orbit Viewer applet at that website which was originally written by Osamu Ajiki (AstroArts) and further modified by Ron Baalke (JPL). We are grateful for useful discussions with D. Fisher, J. Grebowsky, D. Kocevski, and R. Quimby.

References

Acuña, M. H., et al. (2001), Magnetic field of Mars: Summary of results from the aerobraking and mapping orbits, *J. Geophys. Res.*, *106*, 23,403–23,417.

Bougher, S. W., S. Engel, D. P. Hinson, and J. R. Murphy (2004), MGS Radio Science electron density profiles: Interannual variability and implications for the Martian neutral atmosphere, *J. Geophys. Res.*, *109*, E03010, doi:10.1029/2003JE002154.

Brain, D. A. (2007), Global Surveyor measurements of the Martian solar wind interaction, *Space Sci. Rev.*, in press.

Brain, D. A., J. S. Halekas, R. Lillis, D. L. Mitchell, R. P. Lin, and D. H. Crider (2005), Variability of the altitude of the Martian sheath, *Geophys. Res. Lett.*, *32*, L18203, doi:10.1029/2005GL023126.

Cantor, B., M. Malin, and K. S. Edgett (2002), Multiyear Mars Orbiter Camera (MOC) observations of repeated Martian weather phenomena during the northern summer season, *J. Geophys. Res.*, *107*(E3), 5014, doi:10.1029/2001JE001588.

Cho, J. Y. N., and J. Rottger (1997), An updated review of polar mesosphere summer echoes: Observation, theory, and their relationship to noctilucent clouds and subvisible aerosols, *J. Geophys. Res.*, *102*, 2001–2020.

Christou, A. (2005), Predicting Martian and Venusian meteor shower activity, *Earth Moon Planets*, *95*, 425–431.

Connerney, J. E. P., M. H. Acuña, P. J. Wasilewski, G. Kletetschka, N. F. Ness, H. Rème, R. P. Lin, and D. L. Mitchell (2001), The global magnetic field of Mars and implications for crustal evolution, *Geophys. Res. Lett.*, *28*, 4015–4018.

Crider, D. H., D. Vignes, A. M. Krymskii, T. K. Breus, N. F. Ness, D. L. Mitchell, J. A. Slavin, and M. H. Acuña (2003), A proxy for determining solar wind dynamic pressure at Mars using Mars Global Surveyor data, *J. Geophys. Res.*, *108*(A12), 1461, doi:10.1029/2003JA009875.

Crider, D. H., J. Espley, D. A. Brain, D. L. Mitchell, J. E. P. Connerney, and M. H. Acuña (2005), Mars Global Surveyor observations of the Halloween 2003 solar superstorm's encounter with Mars, *J. Geophys. Res.*, *110*, A09S21, doi:10.1029/2004JA010881.

Espley, J. R., P. A. Cloutier, D. H. Crider, D. A. Brain, and M. H. Acuña (2005), Low-frequency plasma oscillations at Mars during the October 2003 solar storm, *J. Geophys. Res.*, *110*, A09S33, doi:10.1029/2004JA010935.

Gurnett, D. A., et al. (2005), Radar soundings of the ionosphere of Mars, *Science*, *310*, 1929–1933.

Liu, J., M. I. Richardson, and R. J. Wilson (2003), An assessment of the global, seasonal, and interannual spacecraft record of Martian climate in the thermal infrared, *J. Geophys. Res.*, *108*(E8), 5089, doi:10.1029/2002JE001921.

McNeil, W. J., R. A. Dressler, and E. Murad (2001), Impact of a major meteor storm on Earth's ionosphere: A modeling study, *J. Geophys. Res.*, *106*, 10,447–10,465.

Mendillo, M., S. Smith, J. Wroten, H. Rishbeth, and D. Hinson (2003), Simultaneous ionospheric variability on Earth and Mars, *J. Geophys. Res.*, *108*(A12), 1432, doi:10.1029/2003JA009961.

Mendillo, M., P. Withers, D. Hinson, H. Rishbeth, and B. Reinisch (2006), Effects of solar flares on the ionosphere of Mars, *Science*, *311*, 1135–1138.

Mitchell, D. L., R. P. Lin, C. Mazelle, H. Rème, P. A. Cloutier, J. E. P. Connerney, M. H. Acuña, and N. F. Ness (2001), Probing Mars' crustal magnetic field and ionosphere with the MGS Electron Reflectometer, *J. Geophys. Res.*, *106*, 23,419–23,427.

Molina-Cuberos, G. J., O. Witasse, J.-P. Lebreton, R. Rodrigo, and J. J. Lopez-Moreno (2003), Meteoric ions in the atmosphere of Mars, *Planet. Space Sci.*, *51*, 239–249.

Morgan, D. D., D. A. Gurnett, D. L. Kirchner, R. L. Huff, D. A. Brain, W. V. Boyton, M. H. Acuña, J. J. Plaut, and G. Picardi (2006), Solar control of radar wave absorption by the Martian ionosphere, *Geophys. Res. Lett.*, *33*, L13202, doi:10.1029/2006GL026637.

Patterson, J. D., T. P. Armstrong, C. M. Laird, D. L. Detrick, and A. T. Weatherwax (2001), Correlation of solar energetic protons and polar cap absorption, *J. Geophys. Res.*, *106*, 149–163.

Patzold, M., S. Tellmann, B. Hausler, D. Hinson, R. Schaa, and G. L. Tyler (2005), A sporadic third layer in the ionosphere of Mars, *Science*, *310*, 837–839.

Pesnell, W. D., and J. Grebowsky (2000), Meteoric magnesium ions in the Martian atmosphere, *J. Geophys. Res.*, *105*, 1695–1707.

Picardi, G., et al. (2005), Radar soundings of the subsurface of Mars, *Science*, *310*, 1925–1928, doi:10.1126/science.1122165.

Safaeilini, A., W. Kofman, J.-F. Nouvel, A. Henrique, and R. L. Jordan (2003), Impact of Mars ionosphere on orbital radar sounder operation and data processing, *Planet. Space Sci.*, *51*, 505–515.

Selsis, F., J. Brillet, and M. Rapaport (2004), Meteor showers of cometary origin in the solar system: Revised predictions, *Astron. Astrophys.*, *416*, 783–789, doi:10.1051/0004-6361:20031724.

Treimann, A. H., and J. S. Treimann (2000), Cometary dust streams at Mars: Preliminary predictions from meteor streams at Earth and from periodic comets, *J. Geophys. Res.*, *105*, 24,571–24,581.

Vaubaillon, J., F. Colas, and L. Jorda (2005), A new method to predict meteor showers: I. Description of the model, *Astron. Astrophys.*, *439*, 751–760.

Wang, J.-S., and E. Nielsen (2003), Behavior of the Martian dayside electron density peak during global dust storms, *Planet. Space Sci.*, *51*, 329–338.

Witasse, O., J.-F. Nouvel, J.-P. Lebreton, and W. Kofman (2001), HF radio wave attenuation due to a meteoric layer in the atmosphere of Mars, *Geophys. Res. Lett.*, *28*, 3039–3042.

Withers, P., and M. Mendillo (2005), Response of peak electron densities in the Martian ionosphere to day-to-day changes in solar flux due to solar rotation, *Planet. Space Sci.*, *53*, 1401–1418.

M. H. Acuña, J. R. Espley, and W. M. Farrell, NASA Goddard Space Flight Center, Code 695, Greenbelt, MD 20771, USA. (jared.espley@gsfc.nasa.gov)

D. A. Brain, Space Sciences Laboratory, University of California, Berkeley, 7 Gauss Way, Berkeley, CA 94720-7450, USA.

B. Cantor, Malin Space Science Systems, Box 910148, San Diego, CA 92191-0148, USA.

D. D. Morgan, Department of Physics and Astronomy, University of Iowa, Iowa City, IA 52242, USA.

G. Picardi, Infocom Department, La Sapienza University of Rome, I-00184 Rome, Italy.

J. Plaut, Jet Propulsion Laboratory, California Institute of Technology, Pasadena, CA 91109, USA.